Catalysis Today 160 (2011) 131–136

Contents lists available at ScienceDirect

Catalysis Today

journal homepage: www.elsevier.com/locate/cattod

Impact of dopants on the sulfation, desulfation and NO_x reduction performance of Ba-based NO_x storage-reduction catalysts☆

Todd J. Toops*, Nathan A. Ottinger, Chengdu Liang, Josh A. Pihl, E. Andrew Payzant

Oak Ridge National Laboratory, 1 Bethel Valley Road, Oak Ridge, TN 37831, USA

ARTICLE INFO

Article history:
Available online 21 September 2010

Keywords:
NO_x storage-reduction (NSR) catalysts
Sulfur
Dopant
Barium
Calcium

ABSTRACT

The performance of a NO_x storage-reduction (NSR) catalyst is strongly dependent on the relative stabilities of nitrates and sulfates on the catalyst surface. This effort studies the effects of introducing 5 mol% La, Ca, and K-dopants into a BaO phase of a model $Pt/Ba/Al_2O_3$ NSR catalyst. The dopants were chosen with a range of properties to affect the BaO lattice spacing and/or the number of oxygen vacancies. The resulting changes in the storage material, in turn, impact the stability of stored nitrates and sulfates, as measured by NO_x conversions and desulfation temperatures. The Ca- and La-doped material shows equivalent or better NO_x reduction performance between 200 and 400 °C, while the K-doped NSR catalyst showed significant decreases in performance at 200 °C but maintained the high performance at 300 and 400 °C. Following the performance measurements, the samples are then sulfated to 5.5 mg S/gcat and desulfated to 1000 °C. All NSR catalysts generally show similar desulfation behavior, but in determining the temperature of 20% sulfur removal ($T_{20\%}$), it is shown that the Ca + Ba sample has a 25 °C lower $T_{20\%}$ than both the Ba-only and La + Ba samples, while K + Ba is 70 °C higher. Additional Ca-based samples were than prepared at the 10, 20 and 100 mol% levels. The higher Ca-doped materials show similar NO_x reduction performance, but the 5% Ca + Ba sample maintains the lowest $T_{20\%}$. Interestingly, the Ca-only sample has a $T_{20\%}$ that is 60 °C higher than the Ba-only NSR catalyst, which indicates that the introduction of 5% Ca into the Ba-lattice has a synergistic effect in lowering the desulfation temperature.

1. Introduction

Lean-burn engines are fundamentally more fuel efficient than engines operating with a stoichiometric fuel/air mixture. A major challenge with these efficient systems is the reduction of NO_x emissions in the lean exhaust. Although several solutions have been demonstrated, each one has drawbacks with respect to cost, implementation, or durability. One of these solutions is the NO_x storage-reduction (NSR) catalyst. It is generally formulated with a NO_x storage component, usually alkali or alkaline earth metal oxides such as Ba or K, and platinum-group metals dispersed over a high surface area γ-alumina washcoat [1,2]. Additionally, commercial-intent NSR catalysts typically contain several other components such as ceria–zirconia for oxygen storage or additives to improve durability [2–5]. Unfortunately, fuel- and lubricant-borne sulfur is also trapped on the storage component in the form of very stable sulfates, diminishing the storage capacity and overall NO_x reduction performance of the NSR catalyst. The sulfates must be removed through periodic high temperature excursions.

The NO_x storage-reduction (NSR) catalyst has shown feasibility in a variety of vehicles [6,7], but the amount of platinum-group metals (PGM) that is required to meet the stringent emissions regulations make these catalysts less attractive. This is especially the case because the high temperatures that these NSR catalysts must endure to maintain functionality results in PGM sintering [5,8–12]. Thus, to meet the durability requirements of the emissions regulations, an even higher PGM loading is required. In moving towards second generation NSR catalysts, it is desirable to reduce the temperature that is required to desulfate the catalysts, while maintaining high NO_x reduction performance over a wide operating window. This performance of NSR catalysts is strongly dependent on the relative stabilities of nitrates and sulfates on the catalyst surface, and to some extent within the bulk of the sample. With typical Ba-based formulations, sulfates are much more stable than nitrates, so sulfur is very effective at poisoning the NO_x storage sites. Further, the high stability of sulfates requires periodic high temperature desulfation to recover the NO_x storage capacity of the catalyst. These high temperature excursions rapidly age the catalyst, adversely impacting NO_x reduction activity [13–16]. The

☆ This paper is for a special issue entitled "Heterogeneous Catalysis by Metals: New Synthetic Methods and Characterization Techniques for High Reactivity", guest edited by Jiolong Gong and Robert Rioux.

* Corresponding author. Tel.: +1 865 946 1207.
E-mail address: toopstj@ornl.gov (T.J. Toops).

0920-5861/$ – see front matter © 2010 Elsevier B.V. All rights reserved.
doi:10.1016/j.cattod.2010.08.009

Table 1
Storage material and dopant properties.

	Ba	Ca	K	La
Covalent radius	1.98 Å	1.74 Å	2.03 Å	1.69 Å
Oxidation state	2+	2+	1+	3+
Expected impact	n/a	Lattice strain	O-vacancies	Ba-vacancies + lattice strain

goal of the present work was to measure the impact of dopants on the NO_x reduction activity and on the stability of sulfates in a model NSR catalyst.

The introduction of dopants can result in three effects on the Ba structure: changes in lattice spacing, oxygen vacancies, or Ba-vacancies. Ba, with a covalent radius of 1.98 Å, is the largest atom that naturally occurs in the 2+ oxidation state, so it is only possible to impart lattice strain through the introduction of smaller atoms. Ca has a 2+ oxidation state but a covalent radius 12% smaller than Ba at 1.74 Å, so it is expected to impart only lattice strain to the Ba-phase. To isolate the impact of introducing oxygen vacancies, an atom of similar covalent radius with a 1+ oxidation state is preferred. K was selected since it has about the same covalent radius, 2.03 Å, and a 1+ oxidation state. Finally, to introduce Ba- or metal vacancies an atom of similar size and a 3+ valence is preferred. Unfortunately, there is not an atom that will consistently have an oxidation state of 3+ that is similar in size to Ba. La was the closest, but since its covalent radius is 1.69 Å, 15% smaller than Ba, it is expected to introduce lattice strain as well as metal vacancies. For reference these effects and parameters are listed in Table 1. Each of these factors is expected to impact the stability of stored nitrates and sulfates, and this impact is the focus of the study as it relates to NO_x conversion and desulfation temperature.

2. Experimental

The NSR catalysts were synthesized in a stepwise fashion. The Pt was dispersed on commercial-grade γ-Al_2O_3 using H_2PtCl_6 and the incipient wetness technique to obtain a 1.5 wt% loading. The storage phases were added to the Pt/Al_2O_3 support using a wet impregnation technique with the corresponding nitrate salts followed by thermal decomposition. The three impregnation solutions were prepared by using 1.28 g of barium nitrate and 10 g of water for each solution; and the dopants in the solutions were 0.025 g of KNO_3, 0.058 g of $Ca(NO_3)_2{\cdot}4H_2O$, and 0.08 g of $La(NO_3)_3{\cdot}xH_2O$ respectively. All of these masses represent a 5 mol% substitution of the Ba metal. 2 g of 1.5 wt% Pt/Al_2O_3 were placed in a 15 cm ID Petri dish and then impregnated with 1 g of nitrate solution. The Petri dish was transferred into a well vented oven that was preheated to 100 °C for removing water. The impregnation/drying cycle was repeated until each impregnation solution was completely loaded onto the Pt/Al_2O_3. After the wet impregnation, the samples were then heated at 2 °C/min to 500 °C in a box furnace and held at this temperature for 2 h to ensure the complete decomposition of nitrates. Samples were taken out of the furnace right after the temperature cooled to 100 °C and stored in a sealed glass vial to avoid adsorption of moisture.

Nitrogen sorption isotherms of the samples were measured at 77 K by using a Micromeritic Gemini 275 system. The specific surface areas were calculated by using the Brunauer–Emmett–Teller (BET) theory based on the adsorption branches of the isotherms. To determine the phases present in the samples, X-ray diffraction was employed. The samples were pretreated at 700 °C mixed with acetone on a zero background tray. A PANalytical X'Pert PRO diffractometer operating at 45 kV and 40 mA with a 0.5° divergence slit, a 1° incident-beam anti-scatter slit, and a 0.5° diffracted-beam anti-scatter slit was used for the primary XRD diffractograms in this study. Scans were taken between 15° and 90° (2θ) with a step size of 0.017° (2θ) and 20 s/step using an X'celerator position-sensitive detector. For the quantitative analysis, additional patterns were recorded using programmable slits for a 2 mm irradiated area on the sample; LaB_6 was used as the internal standard and the XRD patterns were refined through Rietveld refinements. Unit cell parameters were derived from the entire XRD pattern using the PANalytical X'Pert HighScore Plus software program. The techniques applied to acquire the unit cells in this study are expected to be accurate to the fourth decimal place.

To measure NO_x reduction performance of the NSR catalysts, a powder-based microreactor equipped with a Stanford Research System RGA100 (residual gas analyzer) quadrupole mass spectrometer and a fluorescent SO_2 analyzer model 100A from Advanced Pollution Instrumentation was employed. This microreactor has been previously described in detail [5,13]. Briefly, it consists of an 8-mm ID quartz U-tube sample holder with an electronically controlled 4-way valve upstream to enable fast switching from lean to rich conditions. The 4-way valve is equipped with a pressure transducer at each of its outlet streams and a back pressure regulator on the non-reactor line to ensure that the switch from lean to rich is isobaric. This minimizes the impact of switching on the reactor flow and analyzer response. Additionally, since an SO_2 analyzer was employed to monitor all sulfur species, and significant H_2S is expected during desulfation [17–20], a secondary oxidation reactor was employed. Pt/SiO_2 was used to minimize sulfur trapping and the reactor was operated at 700 °C with a constant supply of O_2 (7.5 sccm) added to the 150 sccm coming out of the NSR catalyst reactor. A similar setup for monitoring SO_2 has been used elsewhere [21,22], and they reported a portion of the SO_2 is converted to SO_3 which is not detected by the analyzer. This can be accounted for during calibration as long as the calibration gases are directed through the oxidation reactor. Additionally, the SO_2 analyzer requires ~1 L/min for operation so the effluent is further diluted with 1 L/min of air to ensure that there is enough flow for the instrument.

NO_x reduction measurements were performed at 200, 300, and 400 °C while operating at an approximate space velocity of 30,000 h^{-1}; space velocity is based on the volumetric gas flow at STP and the volume of the powder bed; typical catalyst loadings were 150 mg. The evaluation protocol consisted of a multi-step process as detailed below:

1. Pre-treat freshly loaded catalyst at 700 °C under rich conditions for 8 h.
2. Evaluate initial catalyst NO_x conversion while cycling between lean and rich conditions; begin at 400 °C, followed by 300 °C, and finally 200 °C.
   a. Rich (17 s): 0.71% H_2, 1.19% CO, 5% H_2O, 5% CO_2, balance Ar.
   b. Lean (127 s): 300 ppm NO, 10% O_2, 5% H_2O, 5% CO_2, balance Ar.
   c. NO_x reduction performance evaluated after cycle-to-cycle variation became negligible; typically 1–1.5 h.

   These lean:rich ratios and switching times are based on the guidelines set forth by the Cross-cut Lean Exhaust Emissions Reduction Simulations (CLEERS) protocol for NSR catalysts [23]. An additional 7 s is added to each phase to allow for the experimentally measured rise time associated with the switching from lean to rich.

Table 2
Catalyst composition, initial surface area, and characteristic desulfation temperatures for the Ca-, K-, and La-doped samples.

Catalyst	Pt (wt%)	Ba (mol%)	Dopant (mol%)	Surface area (m^2/g)	$T_{20\%}$ (°C)	Desulfation T	
						$T_{80\%}$ (°C)	$T_{80\%} - T_{20\%}$ (°C)
Pt/Al_2O_3	1.5	–	–	133	–	–	–
Ba-only	1.1	20	0	77	590	772	182
Ca + Ba	1.1	19	1.0	79	565	767	203
K + Ba	1.1	19	1.0	78	661	780	119
La + Ba	1.1	19	1.0	80	588	784	196

3. Sulfate catalyst by introducing 45 ppm SO_2 at 400 °C while cycling between lean and rich conditions. Sulfation was continued until the samples were exposed to a total of 5.5 mg S/g_{cat}.
4. Stop flowing SO_2, switch to rich conditions and wait for the measured SO_2 to decrease below 2 ppm.
5. Desulfate the catalyst in rich conditions while ramping from 400 to 1000 °C at 10 °C/min. Convert released H_2S to SO_2 in oxidation reactor.

For each step, the cycles are allowed to continue until the cycle-to-cycle variation is minimal, typically greater than 1 h. This is as close to a "steady-state" as can be achieved for the inherently dynamic NSR process. Gas flow to the system was controlled using a series of mass flow controllers using pure gases or blends with gas purity levels of 99.999% except for NO (99.0%), CO_2 (99.99%) and SO_2 (99.8%). When using blends the balance gas was always Ar.

3. Results and discussion

The first portion of this study was aimed at evaluating the impact of the dopants Ca, K, or La on Ba-based NSR catalysts. The specific dopant levels are reported in Table 1; it should be noted that the base NSR catalysts is a 20 mol% BaO which corresponds to 27 wt% BaO. XRD on the calcined samples showed that the primary phases present were $BaCO_3$ and $BaAl_2O_4$ and that no independent dopant phases were present (Fig. 1). Further analysis of the diffraction patterns using the Rietveld method allowed the determination of the unit dimensions; the resulting cell volumes are listed in Fig. 1. Since the dopants were either smaller than Ba or would result in vacancies, it was expected that the substitutions would result in smaller lattice dimensions. Indeed, a small decrease in cell size was observed in each of the samples. Additionally, the doped samples all had slightly higher surface areas than the base case, as shown in Table 2, but these differences are statistically insignificant when taking into account sample weighing and the sensitivity of the instrument.

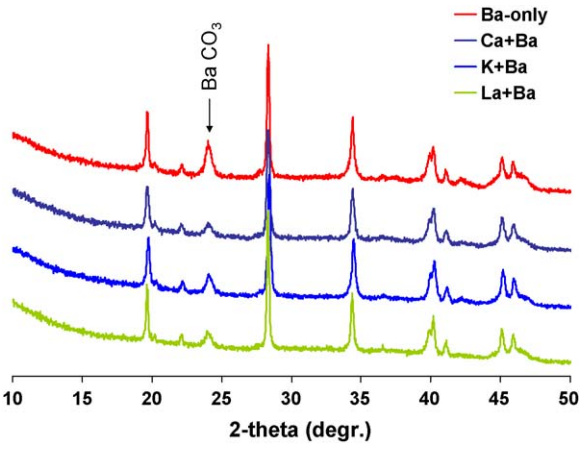

Fig. 1. XRD patterns comparing a Ba-only NSR catalyst with of Ca-, K-, and La-doped samples following 700 °C pretreatment step. Sharp unmarked peaks are indicative of $BaAl_2O_4$.

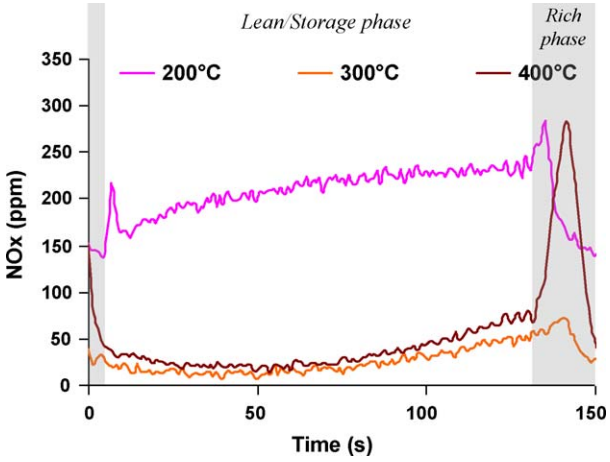

Fig. 2. Typical NO_x profile of NSR catalysts studied during lean-rich cycling. Results are for the Ba-only sample.

While material properties are important to analyze with respect to determining the success of the substitutions, the key metric that we are interested in is NO_x reduction performance and desulfation properties. The NO_x reduction performance was measured under cycling conditions at 200, 300 and 400 °C; results are reported only after the cycle-to-cycle variations were minimal. Typical catalyst outlet NO_x concentration profiles for each temperature are shown in Fig. 2; as described in step 2 above, NO was only introduced during the lean phase. This example is for the Ba-only case. To determine the overall NO_x conversion the following equation was employed:

$$\text{Overall } NO_x \text{ conversion} = \left[\frac{NO_x \text{ stored} - \text{unconverted } NO_x \text{ released}}{NO_x \text{ fed to reactor}}\right] \quad (1)$$

The NO_x stored during the lean phase is the difference between the blank reactor NO_x profile and the experimental NO_x profile during the lean phase. The unconverted NO_x released is calculated from the NO_x measured during the rich phase. Integration of the NO_x effluent profiles reveals that 34%, 86% and 77% of the NO is converted at 200, 300 and 400 °C, respectively. For comparison, the full cycle conversions of the 5% doped Ca, La, and K are shown in Fig. 3. The general trends are the same for each sample with the highest conversions at 300 °C and the lowest at 200 °C.[1] The primary observation in this comparison is that the K + Ba sample has notably poorer NO_x reduction performance at 200 °C; both La + Ba and Ca + Ba samples have essentially the same NO_x conversion as Ba-only. Before discussing the physicochemical implications of these observations, we will analyze the temperature programmed desulfation profiles to gain further insight into sulfate bond strength.

[1] At 300 and 400 °C experimental error is circa ±5%, and at 200 °C error it is expected to be ±10%.

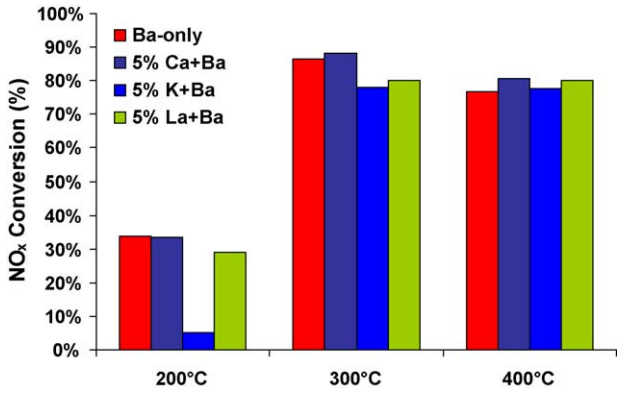

Fig. 3. Comparison of the NO_x conversion for Ba-only NSR catalyst to the Ca-, K-, and La-doped samples at 200, 300, and 400 °C.

While the impact of sulfur on NO_x reduction performance is the primary inhibitor of further deployment of NSR catalyst technology, it can be difficult to measure and compare sulfur tolerance on various catalyst samples. However, the technique and analysis outlined here answers some key questions and allows a fair comparison to be made. As described above, the samples are exposed to the same amount of sulfur and allowed to purge. Temperature programmed reduction follows to 1000 °C. This high temperature is sufficient to remove all of the sulfur and reveal the nature of the stored sulfur, but because it is at such an extreme temperature—well beyond what would normally be expected in an operating vehicle—additional NO_x reduction performance measurements following desulfation are not reasonable. A typical profile of the catalyst outlet sulfur concentration during this sequence is shown in Fig. 4 for the Ba-only case. During the sulfation step, there is a period during which all of the sulfur is adsorbed, followed by the breakthrough during the later cycles. Sulfur is then turned off and the sample is purged, first while cycling, then after switching to rich conditions. When switching to rich conditions, there is typically a significant sulfur release associated with removal of the weakly bound sulfates. After the sulfur level decreases to less then ~10% of the feed value the TPR is started. The TPR profiles are shown in Fig. 5 for each of the Ca-, La-, and K-doped samples.

While visual analysis of these profiles indicates general sulfate stability, a quantitative metric can be used to enable easier comparisons. The $T_{20\%}$ and $T_{80\%}$ columns listed in Table 2 reflect the temperature where 20% and 80% of the total sulfur evolved during the TPR has been released, respectively. The $T_{20\%}$ for Ca + Ba is 25 °C lower than the La + Ba and Ba-only samples, while the K + Ba sample has a $T_{20\%}$ that is 70–95 °C higher than the other samples. Although the sulfur releases at a higher initial temperature, the sulfates that form on K + Ba are much more homogeneous and are released over a narrower temperature window, as there is only a difference of 119 °C between $T_{80\%}$ and $T_{20\%}$. The Ca + Ba and La + Ba behave much more like the Ba-only sample, as a broad desulfation profile is observed with a release profile covering 200 °C. The sharp sulfur release profile of the K + Ba sample results in a $T_{80\%}$ that is within 15 °C of the other samples. There are also some highly stable sulfates observed in the desulfation profiles for both La + Ba and Ca + Ba samples above 900 °C. For the La + Ba sample ~11% of the sulfates are released in a symmetric peak centered at 914 °C. Ca + Ba had a less substantial release of ~5% of the sulfur centered at 924 °C.

While there was not a large shift in the NO_x reduction performance of the doped samples, the significant shifts in sulfur storage and release imply the introduction of the dopants is changing the physicochemical properties of the NSR catalysts. The lower $T_{20\%}$ for the Ca + Ba samples suggests that the introduction of lattice strain from the smaller Ca atoms results in a fraction of the sites having a weaker sulfate bond. Since La + Ba also introduces a smaller atom into the lattice it would be expected that the same effect would be observed, and in Fig. 5 we do see some signs of this less stable sulfate, but as listed in Table 1, the La^{3+} ion also introduces Ba-vacancies. It is possible that the pronounced high temperature peak at 924 °C is due to these metal vacancies, but it also could be due to a simple La_2O_3 phase, which is a known high temperature NO_x reduction catalyst [24–27]. Since K and Ba have very similar covalent radii a lattice strain is not expected, but instead the storage material is expected to have oxygen vacancies. From the dramatic difference in the sulfur release profile compared to Ba-only and the relative homogeneity of the release, it would suggest that dispersion of the K-dopant and the impact on adsorption sites is significant and uniform. Unfortunately, this does not lead to desirable characteristics such as improved NO_x conversion and low temperature sulfur release; however, these attributes could lead to a NSR catalyst for high temperature applications. This observation of higher temperatures is consistent with the previous reports of increased stability with the inclusion of K [28,29].

Because the 5% Ca + Ba sample demonstrated the most promising attributes, i.e. less stable sulfates with equal or better NO_x conversion than Ba-only, additional samples were made with the storage material comprising 10, 20, or 100 mol% Ca. The same fabrication technique outlined above was employed with the specific compositions and surface areas displayed in Table 3. As before, doping the Ba-based NSR catalysts had a minimal impact on the specific surface area, however, for the Ca-only sample, the sur-

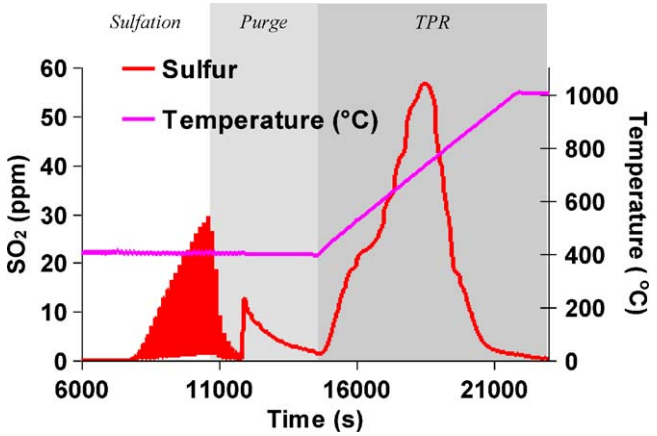

Fig. 4. SO_2 concentrations measured with fluorescence analyzer during a typical sulfation, purge and desulfation experiment. Results are for the Ba-only sample.

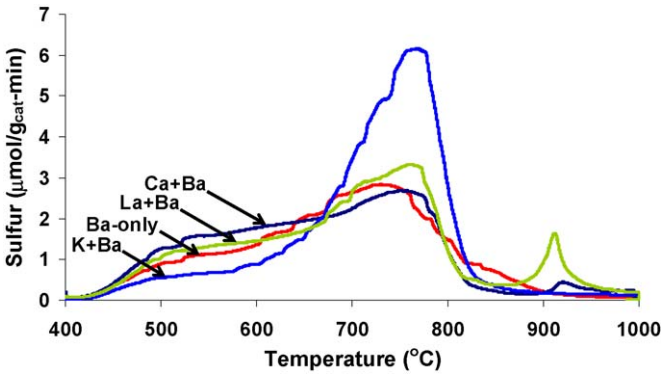

Fig. 5. Temperature programmed reduction (TPR) sulfur release profiles of the sulfated NSR catalysts.

Table 3
NSR catalyst composition, initial surface area, and characteristic desulfation temperatures for the Ca-doped samples.

Catalyst	Pt (wt%)	Ba (mol%)	Ca (mol%)	Surface area (m^2/g)	$T_{20\%}$ (°C)	Desulfation T	
						$T_{80\%}$ (°C)	$T_{80\%} - T_{20\%}$ (°C)
Ba-only	1.1	20	0.0	77	590	772	182
5% Ca + Ba	1.1	19	1.0	79	565	767	203
10% Ca + Ba	1.1	19	2.0	80	596	776	180
20% Ca + Ba	1.1	19	4.0	82	631	783	152
Ca-only	1.1	0.0	20	57	651	757	106

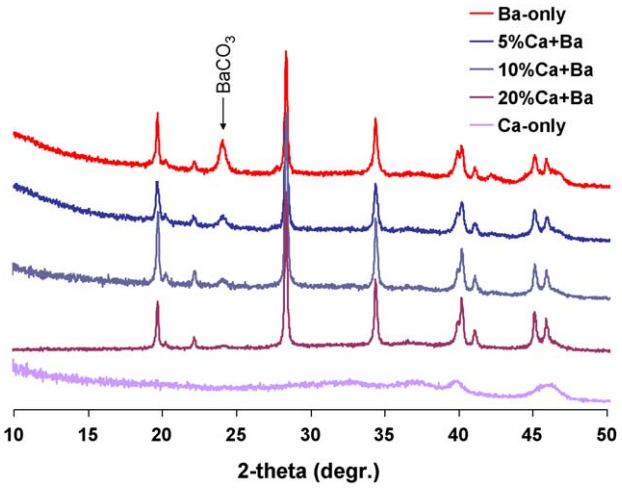

Fig. 6. XRD patterns comparing a Ba-only NSR catalyst with 5%, 10%, 20% and 100% Ca-doped samples following 700 °C pretreatment step. Sharp unmarked peaks are indicative of $BaAl_2O_4$.

face area decreased significantly from 77 to 57 m^2/g. Following a 700 °C pretreatment, XRD was employed to investigate the impact on the Ba-phase and to look for the appearance of other metal oxide phases. The patterns shown in Fig. 6 illustrate that $BaAl_2O_4$ observed in Fig. 1 is present in these samples too, along with the $BaCO_3$ phase that was used to determine the lattice parameters; however, the Ca-only sample does not have any detectable crystalline phases other than γ-Al_2O_3. It should be noted that all of the data presented in this section on the Ba-only and the 5% Ca + Ba samples is the same data presented above in the comparison between Ca, K, and La and is only repeated for comparative purposes.

As before, the key metrics for this study are NO_x reduction performance and desulfation temperature. Fig. 7 shows the NO_x conversion for the five samples, and similar trends are observed for each sample. Except for the 10% Ca + Ba sample, it appears that increasing levels of Ca-substitution lead to higher conversions at 400 °C and possibly 300 °C. For instance, the Ca-only sample has a NO_x conversion of 93% compared to only 79% for the Ba-only sample. This is generally consistent with other reports comparing Ca and Ba storage components in NSR catalysts with the Ca maintaining high NO_x conversion at high temperatures [30]. Considering the surface area of the Ca-only sample is 25% less than any other sample, this suggests significantly different storage and release properties at 400 °C. At 200 and 300 °C, since the conversions are within 6% of each other it is not possible to differentiate the NO_x reduction performance of the samples, but it is still remarkable how well the Ca-only sample compares to the others considering its low surface area. A possible explanation of this improved performance is derived from the XRD pattern of the Ca-only sample. The amorphous Ca phase, suggests a high dispersion and therefore higher coverage of Al_2O_3. This more disperse Ca phase would have a greater propensity to store and release NO_x, i.e. more storage sites would be available at the surface which would also result in a faster release rate. This storage and release relationship is a symbiotic one that is difficult to meaningfully measure independently, and thus is why it is essential to rely on cycling data to effectively compare the different samples.

The same sulfation and desulfation procedure outlined above was followed with these Ca-doped samples. The desulfation TPR profiles are shown in Fig. 8. Once again there is a divergence in sulfate stability between samples. The 10% Ca + Ba sample has essentially the same release profile as Ba-only with a $T_{20\%}$ and $T_{80\%}$ within 6 °C (listed in Table 3). Similar to the K + Ba sample, the 20% Ca + Ba and the Ca-only samples have more stable sulfates and narrower release temperatures. The higher desulfation temperature of 20% Ca + Ba and Ca-only is not surprising considering the improved NO_x reduction at 400 °C for the high Ca-loadings; however, this observation is particularly interesting since 5% Ca + Ba has a lower $T_{20\%}$ then Ba-only. It indicates that the inclusion of a small amount of Ca has a synergistic effect on Ba—the simple addition of a Ca storage phase should increase the sulfate stability, yet it decreases. Although further material characterization is still needed, a plausible explanation of these advantageous effects on sulfate and nitrate stabilities is the changes in lattice structure brought about by dop-

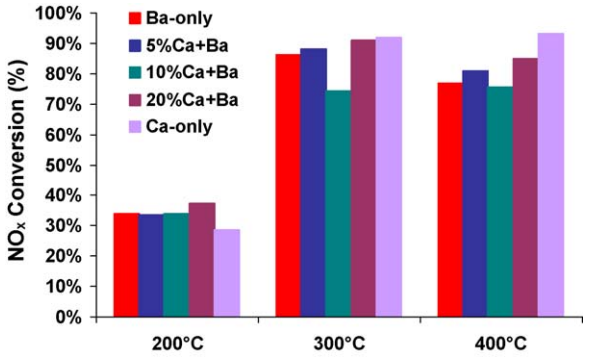

Fig. 7. Comparison of the NO_x conversion for Ba-only NSR catalyst to the Ca-, K-, and La-doped samples at 200, 300, and 400 °C.

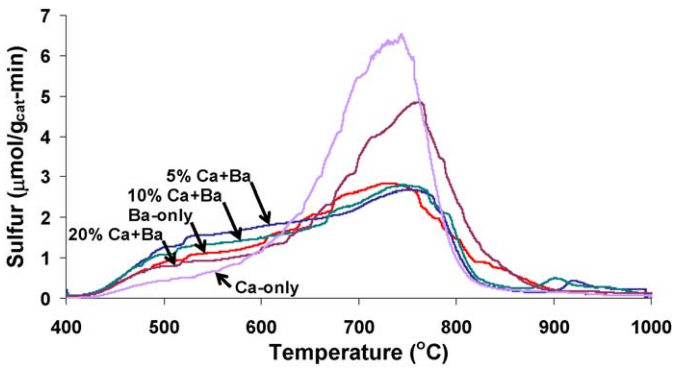

Fig. 8. Temperature programmed reduction (TPR) sulfur release profiles of the sulfated NSR catalysts.

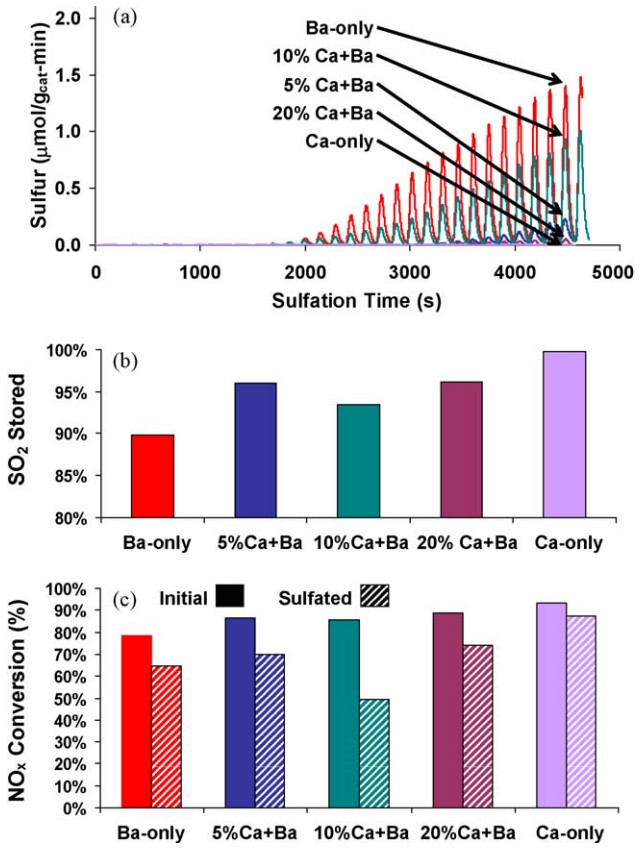

Fig. 9. Sulfur measurements at 400 °C: (a) sulfur breakthrough profiles during sulfation, (b) percentage of sulfur stored that is fed to the reactor, and (c) initial and sulfated NO_x conversion comparison.

ing with a small amount of Ca.

There are other chemical attributes to consider with these samples—particularly with respect to the impact of sulfur on the NO_x reduction. Fig. 9a shows the sulfur breakthrough at 400 °C during the sulfation phase for the entire range of Ba/Ca samples. Since SO_2 is introduced while cycling between lean and rich conditions, this data shows that sulfur is breaking through at varying levels depending on the sample. To quantify this phenomenon, the fraction of the SO_2 introduced to the reactor that is stored is calculated and shown in Fig. 9b. This indicates that the addition of Ca improves the sulfur capture efficiency, with Ca-only storing all of the SO_2 introduced. In general, this would be considered a negative result since this sulfur would detract from the storage sites available for NO_x; however, it is important to take into account how this extra sulfur influences the NO_x reduction. Fig. 9c illustrates the initial NO_x reduction performance at 400 °C, and it can be seen that, although each Ca sample stores more sulfur, the overall NO_x reduction performance is maintained at a high level. In fact, the Ca-only sample has a decrease in NO_x conversion of only 6% compared to 15% for the Ba-only sample; this general observation has also been reported elsewhere [30]. The 5% Ca + Ba and 20% Ca + Ba samples show decreased NO_x conversions similar to Ba-only, 15–16%, but their overall NO_x reduction performance is maintained at a higher level than the Ba-only sample.

4. Conclusions

Introducing metals with the same valence but different radii can benefit both the NO_x reduction performance and desulfation of Ba-based NSR catalysts; however, the electronic manipulation of the storage phase does not necessarily have a positive effect on the NO_x reduction performance or desulfation characteristics, as indicated by the K- and La-doped samples. In the case of equal valent Ca-substitution in the Ba-phase, a synergistic effect was observed; although Ca-only samples adsorb sulfur with high stability, 5% Ca-substitution results in a decrease in sulfate stability on Ba. These promising results will be further explored to investigate if the potential of this approach for manipulating the storage and release properties of NSR catalysts for improved NO_x reduction capabilities and decreased sulfur stability.

Acknowledgements

This research was primarily sponsored by the U.S. Department of Energy, Office of Energy Efficiency and Renewable Energy, Vehicle Technologies Program, with Ken Howden and Gurpreet Singh as the Program Managers. The catalysts were synthesized and characterized at the Center for Nanophase Materials Sciences, which is sponsored at Oak Ridge National Laboratory by the Division of Scientific User Facilities, Office of Basic Energy Sciences, U.S. Department of Energy. Oak Ridge National Laboratory operates under DOE contract number DE-AC05-00OR22725 and is managed by UT-Battelle.

References

[1] N. Miyoshi, S. Matsumoto, K. Katoh, T. Tanaka, J. Harada, N. Takahashi, K. Yokota, M. Sugiura, K. Kasahara, SAE Technical Paper 950809 (1995).
[2] W.S. Epling, L.E. Campbell, A. Yezerets, N.W. Currier, J.E. Parks II, Catal. Rev. Sci. Eng. 46 (2004) 163.
[3] Y. Ji, T.J. Toops, J.A. Pihl, M. Crocker, Appl. Catal. B 91 (1–2) (2009) 329.
[4] Y. Ji, J.-S. Choi, T.J. Toops, M. Crocker, M. Naseric, Catal. Today 136 (2008) 146.
[5] Y. Ji, T.J. Toops, M. Crocker, Catal. Lett. 119 (3–4) (2007) 257.
[6] B.J. Stroia, N.W. Currier, J. Li, R.D. England, J.W. Bush, H. Hess, SAE Technical Paper 2008-01-0769 (2008).
[7] M.V. Twigg, Appl. Catal. B 70 (2007) 2.
[8] Y. Nagai, T. Hirabayashi, K. Dohmae, N. Takagi, T. Minami, H. Shinjoh, S. Matsumoto, J. Catal. 242 (2006) 103.
[9] Y. Ji, T.J. Toops, M. Crocker, Catal. Lett. 119 (2007) 257.
[10] M. Ozawa, Y. Nishio, J. Alloy Compd. 374 (2004) 397.
[11] M. Casapu, J. Grunwaldt, M. Maciejewski, A. Baiker, S. Eckhoff, U. Gobel, M. Wittrock, J. Catal. 251 (2007) 28.
[12] G. Graham, H. Jen, W. Chun, H. Sun, X. Pan, R. McCabe, Catal. Lett. 93 (3–4) (2004) 129.
[13] T.J. Toops, B.G. Bunting, K. Nguyen, A. Gopinath, Catal. Today 123 (2007) 285.
[14] K. Nguyen, H. Kim, B.G. Bunting, T.J. Toops, C.S. Yoon, SAE 2007-01-0470 (2007).
[15] N.A. Ottinger, K. Nguyen, B.G. Bunting, T.J. Toops, J. Howe, SAE Intl. J. Fuels Lub. 2 (1) (2009) 217 (SAE 2009-01-0634).
[16] N.A. Ottinger, T.J. Toops, K. Nguyen, B.G. Bunting, J. Howe, Appl. Catal. B, submitted for publication.
[17] T.J. Toops, J.A. Pihl, Catal. Today 136 (2008) 164.
[18] D.H. Kim, J.H. Kwak, J. Szanyi, X. Wang, G. Li, J.C. Hanson, C.H.F. Peden, J. Phys. Chem. C 113 (2009) 21123.
[19] D.H. Kim, J. Szanyi, J.H. Kwak, X. Wang, J.C. Hanson, M. Hanson, C.H.F. Peden, J. Phys. Chem. C 113 (2009) 7336.
[20] A. Sassi, R. Noirot, C. Rigaudeau, G. Belot, Topics Catal. 30/31 (2004) 267.
[21] L. Kylhammar, P. Carlsson, H.H. Ingelsten, H. Gronbeck, M. Skoglundh, Appl. Catal. B 84 (2008) 268.
[22] D. McLaughlin, F. Meunier, J.P. Breen, R. Burch, 3rd International Taylor Conference, Belfast, N. Ireland, 2004.
[23] S. Pannala, LNT Standard Characterization Protocol, Cross-cut Lean Exhaust Emissions Reduction Simulation (CLEERS), website http://cleers.org/focus_groups/file_list_public.php?group_name=Lean%20NOx%20traps&view_files=&fileid=22, File uploaded May 5, 2006.
[24] X.K. Zhang, A.B. Walters, M.A. Vannice, Appl. Catal. B 4 (2–3) (1994) 237.
[25] T.J. Toops, A.B. Walters, M.A. Vannice, Catal. Lett. 64 (2–4) (2000) 65.
[26] T.J. Toops, A.B. Walters, M.A. Vannice, J. Catal. 214 (2) (2003) 292.
[27] Ch. Sedlmair Ch, K. Seshan, A. Jentys, A. Lercher, J. Catal. 214 (2003) 308.
[28] K. Iwachido, H. Tanada, T. Watanabe, N. Yamada, O. Nakayama, H. Ando, M. Hori, S. Taniguchi, N. Noda, F. Abe, SAE Technical Paper 2001-01-1298 (2001).
[29] D. Dou, J. Balland, SAE Technical Paper 2002-01-0734 (2002).
[30] F. Basile, G. Fornasari, A. Grimandi, M. Livi, A. Vaccari, Appl. Catal. B 69 (2006) 58.